Eur. J. Mineral.
2003, **15**, 309-319

Dedicated to the memory
of Luciano Ungaretti

Lithium in amphiboles: detection, quantification, and incorporation mechanisms in the compositional space bridging sodic and ^{B}Li-amphiboles

ROBERTA OBERTI[1,*], FERNANDO CÁMARA[1], LUISA OTTOLINI[1] and JOSÉ MARIA CABALLERO[2,**]

[1]CNR-Istituto di Geoscienze e Georisorse, sezione di Pavia, via Ferrata 1, I-27100 Pavia, Italy
[2]Departamento de Petrología y Geoquímica, Universidad Complutense de Madrid, Ciudad Universitaria, 28040-Madrid, Spain

Abstract: Lithium is an important constituent in amphiboles, where it can be incorporated up to a limit of three atoms per formula unit (apfu). Lithium can partition itself between the B-group sites (where it occurs at the [6+2]-coordinated M4' position) and the C-group sites (where it occurs at the M3 site). Systematic analysis of the available chemical (EMP + SIMS) and structural data constrains lithium occurrence in amphiboles to the following compositions and exchange vectors: (1) ^{B}Li is incorporated according to $^{M4'}$Li ^{M4}Na$_{-1}$, and no miscibility gap is apparent, despite the difference in the ionic radii; (2) ^{C}Li is incorporated according to ^{M3}Li ^{M2}Fe^{3+} ^{M3}Fe$^{2+}_{-1}$ ^{M2}Fe$^{2+}_{-1}$; however, a partial bond-strength contribution is provided by Si at the T1 site and by Na or K at the A*m* site. Amphiboles with ^{C}Li > 0.5 apfu (root names: leakeite, kornite, whittakerite and pedrizite) have more than half-occupied A-group sites.

Seven new amphibole end-members containing lithium have been discovered in epysienites (dequartzified and albitised granites) from the Pedriza Massif (Central Spain), where lithium incorporation and partitioning is controlled both by the composition of the fluid and the temperature conditions of crystallisation. This occurrence provides an unique opportunity to characterise the $^{M4'}$Li ⇔ ^{M4}Na and ^{M3}Li ⇔ ^{M3}Fe^{2+} solid solutions, as well as model crystal-chemical mechanisms and understand their dependence on intensive parameters.

An accurate quantification and partitioning of lithium in amphiboles is not trivial, and requires a combination of ion-microprobe analysis and structure refinement. Analysis of the available data provides criteria for calculating reliable H_2O and Li_2O values, as well as for obtaining reliable unit formulae from routine EMP results. These criteria can then be used to simplify petrological studies in Li-rich environments.

Key-words: amphibole, lithium, cation partitioning, microanalysis, structure refinement.

1. Introduction

The problem of lithium incorporation and partitioning in amphiboles could be addressed in the last ten years due to the advent of suitable *in situ* microanalytical procedures (ion-microbe analysis by secondary-ion mass spectrometry, SIMS). Since the late 1950s, lithium was known to occur as the major B (M4 site) cation in holmquistite and clinoholmquistite, minerals which occur in Li-rich pegmatites. In the 1990s, lithium was found to be a rather common constituent in sodic amphiboles from both peralkaline granites and manganese-rich metasediments. In these environments, lithium is almost exclusively incorporated into the octahedral C-group sites, where it orders at the M3 site. A discussion of how the presence of octahedral lithium may affect petrologic studies is reported in Hawthorne *et al*. (1993, 1994), and a complete list of the published papers on Li-bearing amphiboles is reported in Caballero *et al.* (2002). In the last few years, detailed petrologic and mineralogical work has been carried out on monoclinic Li-rich amphibole from epysienites from the Pedriza Massif (Sierra de Guadarrama, Spain), in which lithium occurs both at the B- and C-group sites. This has led to the discovery of seven new Li-bearing end members (four of which are cited here for the first time). More interestingly, this work has provided further insights onto the compositional space for lithium incorporation in amphiboles, which was found to encompass the Mg-Fe-Mn-Li and the sodic group *via* the ^{B}LiNa$_{-1}$ exchange vector (Oberti *et al.*, 2000; Caballero *et al.*, 2002).

The first aim of the present paper is to describe in detail the continuous solid solution between ^{B}Li and ^{B}Na in amphiboles (relevant root-names and ideal formulae in Table 1), as well as link the exchange vectors involving lithium to petrogenetic conditions. Systematic ion-microprobe analysis of lithium in amphiboles remains problem-

*E-mail address: oberti@crystal.unipv.it **Present address: C/Cruces 24, E-06420 Castuera, Badajoz, Spain

0935-1221/03/0015-0309 $ 4.95
DOI: 10.1127/0935-1221/2003/0015-0309

Table 1. Root-names and ideal formulae of the amphibole end-members that can incorporate lithium. The other end-member names can be obtained by combination with the prefix sodic, ferro, ferri and fluoro.

Root name	Ideal formula
clinoholmquistite	$^{A}\square\ ^{B}Li_2\ ^{C}[Mg_3\ Al_2]\ ^{T}Si_8\ O_{22}\ ^{X}(OH)_2$
pedrizite	$^{A}Na\ ^{B}Li_2\ ^{C}[Mg_2\ Al_2\ Li]\ ^{T}Si_8\ O_{22}\ ^{X}(OH)_2$
whittakerite*	$^{A}Na\ ^{B}(Na, Li)_2\ ^{C}[Mg_2\ Al\ Fe^{3+}\ Li]\ ^{T}Si_8\ O_{22}\ ^{X}(OH)_2$
winchite	$^{A}Na\ ^{B}(Ca\ Na)\ ^{C}(Mg_4\ Al)\ ^{T}Si_8\ O_{22}\ ^{X}(OH)_2$
leakeite	$^{A}Na\ ^{B}Na_2\ ^{C}(Mg_2\ Fe^{3+}{}_2\ Li)\ ^{T}Si_8\ O_{22}\ ^{X}(OH)_2$
kornite	$^{A}Na\ ^{B}Na_2\ ^{C}(Mg_2\ Mn^{3+}{}_2\ Li)\ ^{T}Si_8\ O_{22}\ ^{X}(OH)_2$
arfvedsonite	$^{A}Na\ ^{B}Na_2\ ^{C}(Fe^{2+}{}_4\ Fe^{3+}{}_2)\ ^{T}Si_8\ O_{22}\ ^{X}(OH)_2$
eckermannite	$^{A}Na\ ^{B}Na_2\ ^{C}(Mg_4\ Al)\ ^{T}Si_8\ O_{22}\ ^{X}(OH)_2$
riebeckite	$^{A}\square\ ^{B}Na_2\ ^{C}(Fe^{2+}{}_3\ Fe^{3+}{}_2)\ ^{T}Si_8\ O_{22}\ ^{X}(OH)_2$

*The root name has been approved by IMA-CNMMN for crystal 1, but the compositional field is still under debate: $1.0 < {}^{B}Na < 1.5$ apfu and $0.5 < {}^{B}Li < 1.5$ apfu (Leake *et al*,. 1997), or $0.5 < {}^{B}Li < 1.5$ apfu (pending proposal; Leake, pers. com.).

atic. Accurate quantification must rely on careful calibration by matrix-matched standards, which are rarely available, and/or on correction of complex matrix effects on ion yields, which are in most cases unpredictable. SIMS analyses are also not easily accessible, expensive and often very time-consuming. Therefore, a further aim of this study is to provide diagnostic markers of the presence of lithium in amphiboles, as well as simple crystal-chemical constraints that can be applied to routine electron-microprobe data in order to estimate lithium content and partitioning in a reliable way.

These topics are particularly suitable for dedication to Luciano Ungaretti, in recognition of his fundamental contribution to amphibole crystal-chemistry. At the beginning of the work leading to the latest report on amphibole nomenclature (Leake *et al*., 1997), Luciano proposed a classification scheme based on charge arrangement, that would have effectively highlighted the stringent analogies between ^{B}Na- and ^{B}Li-amphiboles. Also, most of his work was devoted to showing that structure refinement is a very powerful and site-specific analytical method, which is one of the keynotes of the present paper.

2. Experimental and analytical procedures

2.1 Occurrence and petrology

The ^{B}Li clinoamphiboles studied here were found in episyenites from the Eastern Pedriza Massif (Sierra de Guadarrama, Central System, Spain), which replace a cordierite-bearing porphyritic monzogranite. Each episyenitic body is a discrete tabular structure, up to several metres wide and tens of metres long. They are generally oriented N100ºE, and irregularly distributed over an area of 1.5 × 0.8 km centred on Fuente Grande (Villaseca & Pérez-Soba, 1989).

Although strongly enriched in lithium, these episyenites share the petrological and structural features of the more common mafic (Fe-Ca) episyenites from the Sierra de Guadarrama. They are all metasomatic rocks derived from granitoid protoliths by quartz dissolution and alkali metasomatism (usually sodic but sometimes also potassic), which occurred about 277 Ma ago (Early Permian) during a regional hydrothermal event controlled by extensional tectonics (Caballero, 1993). Episyenites from Sierra de Guadarrama are not structurally or geochronologically related to the late Hercynian magmatic episodes (González-Casado *et al*., 1996).

Geochemical data and fluid inclusions in calcic minerals (pyroxenes and epidotes) suggest that episyenites formed by pervasive interaction with meteoric aqueous fluids of low to moderate salinity (< 12 wt% NaCl equiv., and CO_2 below detection limit), which percolated along fracture bands at pressures not exceeding 150-170 MPa, and at an average *T* close to 520ºC (by stable isotopes thermometry). Fluids originally in equilibrium with the granitoid protoliths were probably channelled along fracture bands; they rose to shallower depth and reacted with the granite body under decreasing temperatures. All the evidence suggests a large amount of fluids, with a flux rate dominant over the fluid-rock reaction rate during the metasomatic event (Caballero, 1999).

The episyenitic alteration preserves the original porphyritic texture of the granitoid protolith. Magmatic feldspar-armoured biotite, plagioclase cores, K-feldspar and zircon are sporadically preserved. Relict phenocrysts of zoned plagioclase, largely replaced by hydrothermal albite, are embedded in a matrix of xenoblastic albite and fine-grained intergranular aggregates of albite, aegirine, aegirine-augite, titanite, magnetite, apatite ± andradite, and a mixture of ^{B}Li-clinoamphiboles after pyroxene.

The studied amphiboles were collected in two episyenitic bodies, the first located in the Arroyo de la Yedra Valley [codes C2, C4, C20 and C24 in this work, and C3 in Oberti *et al.* (2000)], and the second at Fuente Grande, 500 m NE from the former (code C5). The two outcrops mainly differ in terms of composition and texture of the amphiboles. In episyenites from Arroyo de la Yedra, amphiboles are quite homogeneous, with ^{B}Li in the range 0.5-2.0 atoms per formula unit (apfu) and low Zn contents. In episyenites from Fuente Grande, the B-site composition also encompasses that of sodic amphiboles, while the Zn contents are generally higher (> 2.0 wt%) and similar to those of biotites from the granitoid protolith. Amphibole crystals are generally very heterogeneous, and are characterised by complex zoning and replacement textures, with widespread sealed intragranular fractures and zoning (Na-rich cores and Na-poor rims and fracture zones).

The marked decrease in the Na and Mg contents along core-to-rim traverses, as well as the presence of relict aegirine-augite of episyenitic origin, all suggest progressively decreasing temperature during the episyenitic alteration process. Both the studied outcrops are weakly affected by the late-stage hydrothermal processes, which in this area occurred at lower temperatures, and led to the following mineral associations: 1) tainiolitic mica and microcline, 2) quartz, ferro-actinolite and chlorite, and 3) sericite, hematite, kaolinite and clinozoisite.

2.2 Electron- and ion-microprobe analysis

Systematic wavelength-dispersive analyses on grain-mount thin sections were obtained with a JEOL-8900M electron-microprobe at the Universidad Complutense of Madrid. Standard operating conditions used were excitation voltage of 15 kV, specimen current of 20 nA, peak-count time of 10 s and background-count time of 5 s. The following standards and crystals were used for *K*α X-ray lines: Si: albite (PET); Ti and Ca: kaersutite (PET); Al: sillimanite (TAP); Fe and Mn: almandine (LiF); Mg: kaersutite (TAP); Zn: gahnite (LiF); Na: albite (TAP); K: microcline (PET); F: apatite (TAP). Data reduction was performed with the CITZAF software package (Armstrong, 1988). For some samples (C3, C4, C20, and C24), a mineral concentrate was also analysed for Fe_2O_3 by redox titration. The purity of this concentrate was estimated to be higher than 99 ± 2 % from modal analysis; the major impurity was ferro-actinolite, which intimately replaces most of the amphibole.

Electron microprobe analyses were performed on the refined crystals and on crystals selected on thin sections using an ARL microprobe at the Università di Modena, Italy. In these samples, EMP and SIMS analyses (see below) were carried out on the same micro-areas, so as to minimise the effects of compositional zoning that was very significant in some samples. We should note, however, that the volumes sampled by EMPA and SIMS did not match exactly, mainly due to physical reasons (*e.g.*, the different diameter of the ion and electron beams, the different sample-thickness involved in the production of secondary-ions and X-rays). These features may lead to further problems in the analysis of complex zoned samples in which light elements occur as minor constituents. Analytical conditions were 15 kV accelerating voltage, 20 nA beam current and a peak-count time of 10 s. The following standards and crystals were used for *K*α X-ray lines: Si, Ca and Mg: clinopyroxene (ADP, PET, and RAP, respectively); Ti and Fe: ilmenite (PET, LiF); Al: sillimanite, TAP; Fe and Mn: ilmenite (LiF, PET); Al and Mn: spessartine (RAP, LiF); Na: albite (RAP); K: microcline (PET); F: fluorite (RAP); Zn: Zn100 % (LiF); V, V100 % (LiF). Data were processed using the PROBE 5.2 program (Donovan & Rivers, 1990).

SIMS analyses for light elements (H, Li, B, F) were performed on the refined crystals and on 17 critical compositions obtained by the preliminary EMP work in Madrid. Analyses were done with a Cameca IMS 4f ion microprobe (CNR-IGG, Pavia) with an $^{16}O^-$ primary beam ~ 10 μm ∅, corresponding to a beam current of ~ 4 nA. Secondary positive-ion currents were measured at masses 1 (H), 7 (Li), 11 (B), 19 (F) and 30 (Si, used as the reference element), and corrected for isotopic abundance. Matrix effects on H ion-yield due to the presence of Si and Fe (+ Mn) were also corrected for using empirical calibration curves (Ottolini & Hawthorne, 2001). The accuracy of SIMS analysis for H_2O is expected to be ~ 10 % rel. B ion signals, tested at mass number 11 (amu) were negligible. Li analysis is complicated by unpredictable matrix effects related to the high SiO_2 and FeO_{tot} contents. Detailed analytical procedures are described in Ottolini *et al*. (1993) and in Ottolini & Oberti (2000). In the present case, however, the lack of matrix-matched standards, prevented a direct calculation of the accuracy for Li, which was estimated to be around 10-15 % rel. for all the samples. F was quantified following the SIMS procedure described in Oberti *et al.* (2000). Also in this case, we estimated a level of accuracy of the order of ~ 10 % rel.

2.3 X-ray data collection and structure refinement

Around 40 amphibole crystals selected from mineral separates were mounted on a Philips PW-1100 four-circle diffractometer, and examined with graphite-monochromatized Mo*K*α X-radiation; crystal quality was assessed *via* profile analysis of Bragg diffraction peaks. Unit-cell dimensions were calculated from least-squares refinement of the *d* values obtained from 50 rows of the reciprocal lattice by measuring the gravity centroid of each reflection and its corresponding antireflection in the θ range –30° to 30°. Due to their small size, samples 2 (C5C n. 3) and 3 (C5A n. 5) were examined with a Bruker AXS D8 diffractometer equipped with a Smart Apex CCD detector and working with graphite-monochromatised Mo*K*α X-radiation. For sample 2, a crystal-to-detector distance of 4 cm was used to record four batches of 840 images (10 s each, angular increment of 0.2°) at 90° ω rotation at different phi values. For sample 3, three batches of 180 images (5 s each, angular increment of 1°) at 120° rotation were recorded. The SMART software version 5.55 was used for data collection, and the SAINT+ software version 6.02 (® Bruker AXS) was used to integrate the diffracted intensities. Unit-cell dimensions were calculated from least-squares refinement of the position of all the collected reflections.

Intensity data were collected for 13 selected representative crystals in the range $2° < \theta < 30$-$38°$ (Table 2). Four to five monoclinic equivalents were collected with the Bruker Smart Apex detector; only the monoclinic pairs *hkl* and *h-kl* were collected with the Philips PW1100 detector. Intensities (*I*) were corrected for absorption, Lorentz and polarisation effects, and then averaged and reduced to structure factors (*F*). The high R_{sym} values obtained for samples 1 and 4 are due to the small size and low quality of the crystals, which are often zoned in rock sample C5.

Reflections with $I > 3\ \sigma_I$ were considered as observed during unweighted full-matrix least-squares refinement on *F*. Scattering curves for fully ionized chemical species were used at those sites where chemical substitutions occur; neutral *vs.* ionized scattering curves were used at the

Table 2. Sample codes, crystal data and selected refinement information for the samples studied here (arranged in order of increasing Li_2O content).

n.	Sample code	SEQ	*a* (Å)	*b* (Å)	*c* (Å)	β (°)	*V* (Å^3)	θ_{max} (°)	R_{sym} %	R_{obs} %	R_{all} %	# F_{all}	# F_{obs}
1	C5C n. 2	975	9.712(9)	17.851(23)	5.297(2)	103.63(5)	892.5	30	10.8	4.0	8.4	1353	756
2	C5C n. 3	1048	9.594(1)	17.856(2)	5.285(1)	102.94(3)	882.3	38	3.6	5.8	6.5	2364	1238
3	C5A n. 5	1041	9.535(3)	17.876(6)	5.294(2)	102.54(1)	880.9	33	4.6	5.1	8.3	1646	1118
4	C5C2 n. 2	987	9.570(13)	17.884(19)	5.289(6)	102.59(8)	883.5	30	8.9	5.1	7.7	1339	915
5	C24 n. 2	950	9.510(5)	17.854(8)	5.293(4)	102.30(5)	878.2	30	1.5	1.9	2.6	1338	1142
6	C2B n. 8	1043	9.462(6)	17.898(9)	5.302(3)	101.88(4)	878.6	35	2.1	2.2	3.3	2002	1709
7	C2A n. 3	1040	9.483(3)	17.904(5)	5.302(2)	101.96(2)	880.7	35	1.1	1.7	2.4	2005	1852
8	C2A n. 1	1037	9.488(3)	17.859(5)	5.295(2)	102.04(2)	877.4	35	1.5	1.8	2.5	2002	1707
9	C2B n. 5	1042	9.491(3)	17.857(7)	5.292(2)	102.11(3)	877.0	35	1.3	1.6	2.1	1996	1895
10	C2A n. 2	1039	9.496(4)	17.883(8)	5.297(2)	102.06(3)	879.6	35	1.2	1.6	2.2	2006	1892
11	C2B n. 4	1034	9.483(3)	17.836(6)	5.289(2)	102.14(3)	874.7	30	2.6	2.1	2.7	1330	1280
12	C4 n. 3	952	9.501(4)	17.856(8)	5.294(3)	102.10(4)	878.2	30	0.9	1.6	2.0	1337	1222
13	C24 n. 3	951	9.508(4)	17.862(6)	5.294(3)	102.24(3)	878.6	30	1.5	1.5	2.3	1340	1112

Note: SEQ is the sequence number in the CNR-IGG-PV amphibole database; *R* are the standard disagreement indices calculated for the corrected intensities of equivalent monoclinic reflections (R_{sym}), and for the observed and calculated structure factors (*F*) of all the reflections (R_{all}) and of those used for the refinement ($I > 3\sigma_I$, R_{obs}).

T and anion sites (except O3). Selected crystal data and refinement information for the representative samples selected for this work, which all belong to the *C*2/*m* space group, are given in Tables 2 and 3. Atom positions and displacement parameters are given in Table 4 (deposited; it can be obtained through the E.J.M. Editorial Office – Paris or from the authors). Complete refinement results and mineral data for the four new end-members (samples n. 1, 3, 6, and 10) will be published separately. Observed and calculated structure factors are available from the authors (R.O. and F.C.) upon request (or through the E.J.M. Editorial Office – Paris).

3. Calculation of the unit formulae

For all the amphibole compositions (around 50) for which complete (EMP + SIMS) analyses were available, unit formulae were calculated on the basis of 24 (O, OH, F) pfu. The sum of the OH and F contents was always very close (± 1 %) to the ideal value of 2.0 apfu, thus confirming the accuracy of the SIMS analyses, and excluding the presence of significant dehydrogenation. Therefore, partial dehydrogenation in Li-rich amphiboles has so far only been found in some samples crystallised within oxidative trends in silica-saturated peralkaline granites (Hawthorne *et al.*, 1993). The short and nearly constant values measured for the <T1-O> distance (1.617-1.620 Å) preclude the presence of tetrahedral Al in all the samples studied here (Oberti *et al.*, 1995), likewise in the other refined amphiboles from the Pedriza Massif and in most of the previously studied Li-rich amphiboles. Therefore, the Fe^{3+}/Fe^{2+} ratios in the unit formulae were slightly varied so as to obtain 8.0 Si apfu. The amount of lithium entering the octahedral sites was then calculated according to

Table 3. Selected refinement results [mean bond lengths (Å), interatomic angles (°), and site scattering value (ss, epfu)] for the Li-rich amphiboles studied here.

n.	T1-O	T2-O	M1-O	M2-O	M3-O	$^{[8]}$M4-O	$^{[6]}$M4'-O	A*m*-O	O6-O7-O6	ss M1	ss M2	ss M3	ss O3
1	1.619	1.631	2.074	2.021	2.120	2.522		2.805	111.1	33.28	50.17	8.92	17.28
2	1.618	1.624	2.083	2.013	2.101	2.502		2.782	110.4	35.65	50.40	12.50	16.84
3	1.616	1.624	2.090	2.014	2.110	2.490	2.331	2.776	111.0	35.90	49.70	14.88	16.64
4	1.620	1.625	2.094	2.017	2.111	2.491	2.339	2.773	111.0	36.18	50.69	14.19	16.99
5	1.619	1.625	2.086	2.014	2.106	2.497	2.325	2.767	110.6	30.76	49.63	11.17	17.01
6	1.619	1.624	2.104	2.010	2.109	2.511	2.290	2.774	111.4	37.62	48.93	17.11	16.43
7	1.618	1.625	2.104	2.012	2.113	2.507	2.301	2.773	111.2	38.01	49.62	16.28	16.53
8	1.618	1.625	2.098	2.008	2.110	2.479	2.300	2.767	111.1	33.87	48.98	13.33	16.81
9	1.618	1.625	2.095	2.010	2.107	2.484	2.305	2.767	110.9	32.87	49.28	12.74	16.88
10	1.619	1.625	2.101	2.009	2.113	2.482	2.297	2.770	111.2	35.88	49.33	14.27	16.63
11	1.617	1.625	2.090	2.009	2.106	2.509	2.296	2.763	110.7	31.20	49.03	11.49	16.92
12	1.619	1.626	2.094	2.010	2.105	2.502	2.307	2.766	110.8	32.83	49.74	11.68	16.88
13	1.619	1.626	2.091	2.012	2.106	2.500	2.317	2.769	110.7	31.78	49.78	12.16	16.86

Note: the refined site-scattering values at the A- and B-group sites are reported in Table 5

Table 5. Chemical analyses (EMPA + SIMS) and unit formulae [on the basis of 24 (O + F) and 8 Si apfu] of the refined amphiboles (a) and of other 17 representative points from thin sections (b).

Table 5a.

	1	2	3	4	5	6	7	8	9	10	11	12	13
SiO_2	54.26	54.26	55.25	55.16	56.86	56.11	56.32	56.61	56.50	56.81	57.20	56.07	57.14
TiO_2	1.07	0.84	0.52	0.79	1.01	0.07	0.46	1.06	0.86	1.35	0.78	0.98	0.89
Al_2O_3	0.57	0.63	0.60	0.77	1.30	1.51	1.27	1.26	1.19	1.24	1.69	1.37	1.45
Fe_2O_3	13.36	14.84	15.7	15.65	13.95	15.63	15.96	14.61	14.44	14.34	13.89	14.23	14.06
FeO	4.68	5.72	7.61	7.26	8.03	12.98	13.26	10.33	9.41	12.9	9.05	9.27	9.55
MnO	0.97	1.05	1.08	1.26	0.63	1.14	0.77	0.78	0.70	0.59	0.63	0.93	0.60
MgO	6.69	5.88	6.28	5.38	7.23	5.04	4.16	5.50	6.36	4.32	6.63	5.45	6.11
ZnO	3.66	4.08	2.90	3.17	0.18	0.21	0.20	0.19	0.17	0.08	0.18	0.25	0.11
Li_2O_{SIMS}	2.28	2.50	2.84	3.12	3.74	3.80	4.10	4.31	4.33	4.45	4.47	4.47	4.69
CaO	0.67	0.48	0.41	0.23	0.47	0.13	0.12	0.18	0.27	0.18	0.39	0.25	0.30
Na_2O	6.71	5.08	3.84	4.02	3.86	1.29	1.92	2.62	2.52	2.42	2.49	2.93	2.64
K_2O	0.72	0.64	0.40	0.29	0.21	0.01	0.07	0.17	0.16	0.17	0.11	0.21	0.16
F_{SIMS}	1.55	1.93	1.03	0.86	1.64	0.54	1.17	1.26	1.32	1.17	1.42	1.54	1.60
H_2O_{SIMS}	1.32	1.14	1.57	1.64	1.37	1.88	1.53	1.51	1.54	1.55	1.50	1.36	1.40
O=F	0.65	0.81	0.43	0.36	0.69	0.23	0.49	0.53	0.56	0.49	0.69	0.65	0.67
Total	97.86	98.26	99.60	99.24	99.79	100.11	100.82	99.86	99.21	101.08	99.74	98.66	100.03
Si	8.00	8.00	8.00	8.00	8.00	8.00	8.00	8.00	8.00	8.00	8.00	8.00	8.00
Al	0.10	0.11	0.10	0.13	0.22	0.26	0.22	0.22	0.20	0.21	0.28	0.23	0.24
Mg	1.47	1.29	1.35	1.16	1.52	1.06	0.87	1.17	1.34	0.92	1.38	1.16	1.28
Ti	0.12	0.09	0.06	0.09	0.11	0.01	0.05	0.11	0.09	0.14	0.08	0.10	0.09
Fe^{2+}	0.58	0.71	0.92	0.88	0.94	1.55	1.58	1.22	1.11	1.52	1.06	1.11	1.12
Fe^{3+}	1.48	1.65	1.71	1.71	1.48	1.68	1.71	1.55	1.54	1.52	1.46	1.53	1.48
Mn^{2+}	0.12	0.13	0.13	0.15	0.07	0.14	0.09	0.09	0.08	0.07	0.08	0.11	0.07
Zn^{2+}	0.40	0.44	0.31	0.34	0.02	0.02	0.02	0.02	0.02	0.01	0.02	0.03	0.01
Li	0.73	0.58	0.42	0.54	0.64	0.28	0.46	0.62	0.62	0.63	0.64	0.73	0.71
Sum C	5.00	5.00	5.00	5.00	5.00	5.00	5.00	5.00	5.00	5.00	5.00	5.00	5.00
Li	0.62	0.90	1.24	1.28	1.48	1.90	1.88	1.83	1.85	1.89	1.88	1.84	1.94
Ca	0.11	0.08	0.06	0.04	0.07	0.02	0.02	0.03	0.04	0.03	0.06	0.04	0.05
Na	1.27	1.02	0.70	0.68	0.45	0.08	0.1	0.14	0.11	0.08	0.06	0.12	0.01
Sum B	2.00	2.00	2.00	2.00	2.00	2.00	2.00	2.00	2.00	2.00	2.00	2.00	2.00
Na	0.64	0.43	0.38	0.45	0.60	0.28	0.43	0.58	0.58	0.58	0.61	0.69	0.71
K	0.13	0.12	0.07	0.05	0.04	0.00	0.01	0.03	0.03	0.03	0.02	0.04	0.03
Sum A	0.77	0.55	0.45	0.5	0.64	0.28	0.44	0.61	0.61	0.61	0.63	0.73	0.74
F	0.72	0.90	0.47	0.39	0.73	0.24	0.53	0.56	0.59	0.52	0.63	0.70	0.71
OH	1.30	1.12	1.51	1.59	1.29	1.79	1.45	1.43	1.46	1.46	1.40	1.30	1.31
Sum O3	2.02	2.02	1.98	1.98	2.02	2.03	1.98	1.99	2.05	1.98	2.03	2.00	2.02
O.S.	0.72	0.70	0.65	0.66	0.61	0.52	0.52	0.56	0.58	0.50	0.58	0.58	0.57
ss C_{cal}	92.33	98.44	101.01	100.50	90.71	105.36	104.29	95.93	94.02	99.71	92.00	93.59	92.24
ss B_{cal}	18.03	15.52	12.62	12.12	10.79	6.98	7.14	7.63	7.56	7.15	7.50	7.64	7.04
ss A_{cal}	9.51	7.01	5.51	5.90	7.36	3.08	4.92	6.95	6.95	6.95	7.09	8.35	8.38
ss tot_{cal}	119.87	120.97	119.14	118.52	108.86	115.42	116.35	110.51	108.53	113.81	106.59	109.58	107.66
ss C_{ref}	92.36	98.55	100.48	101.06	91.57	103.65	103.91	96.17	94.88	99.49	91.72	94.27	93.71
ss B_{ref}	17.59	14.61	12.01	11.14	8.54	6.89	5.87	6.84	6.90	6.55	7.51	6.84	7.56
ss A_{ref}	8.21	6.86	5.15	6.07	6.98	3.96	4.97	6.08	6.11	5.82	6.93	6.81	6.48
ss tot_{ref}	118.16	120.02	117.64	118.27	107.09	114.50	114.75	109.09	107.89	111.86	106.16	107.92	107.75

O.S. = oxidation state = Fe^{3+}/Fe_{tot}. Table 5a compares refined (ref) and calculated (cal) group-site scattering values (ss); Table 5b compares Li_2O and H_2O values measured (SIMS) and estimated (est) with the method proposed in this study.

$^{C}Li = 5 - (Mg + Al + Ti + Mn + Fe^{2+} + Fe^{3+} + Zn)$. The remaining lithium was assigned to the B-group sites, together with Ca and Na = $2 - (^{B}Li + Ca)$. Analytical data and unit-formulae are reported in Table 5. The group-site scattering values derived from these unit formulae are in close agreement with the refined values (average difference 1 %, maximum difference 1.7 %; Table 5a), this being a measure of the quality of the two independent analyses.

The 17 (EMP + SIMS) analyses performed on selected points in thin sections were treated in the same way as analyses of the refined crystals (Table 5b). On the whole, all the crystal-chemical constraints discussed above are respected. However, in some cases some oddities can be observed. This is particularly the case of intensely zoned crystals, where a small displacement between the EMP and SIMS analytical spots can produce a serious bias. This effect is less important in the refined crystals, where averaging over many spots allows a better fit with the averaged composition given by the structure refinement. For instance, in some points the value of the oxidation state

Table 5b.

	C24 1	C24 2	C24 3	C24 4	C24 5	C24 6	C5 7	C5 8	C5 9	C5 10	C5 11	C20 12	C20 13	C20 14	C20 15	C20 16	C20 17
SiO_2	54.70	55.59	56.33	55.70	55.67	55.84	55.26	54.97	55.65	54.18	54.77	55.01	55.62	55.69	56.04	56.14	56.14
TiO_2	1.32	0.82	0.81	1.53	0.89	1.11	0.22	0.40	0.49	0.47	0.89	0.82	1.87	2.20	1.43	1.61	1.52
Al_2O_3	1.21	0.99	1.30	1.14	0.93	1.28	0.49	0.52	0.71	0.41	0.69	1.58	1.63	0.99	1.36	1.36	1.41
Fe_2O_3	14.07	13.72	13.51	15.70	17.82	17.58	17.65	17.84	20.44	20.00	13.71	12.59	12.80	15.11	11.10	10.98	13.84
FeO	9.94	9.70	8.45	8.66	4.01	6.15	7.47	4.53	1.82	2.00	4.56	12.78	12.48	10.26	14.38	14.82	11.97
MnO	0.74	0.69	0.67	0.68	0.56	0.55	1.15	1.04	1.07	1.13	0.66	0.74	0.78	0.73	0.64	0.65	0.62
MgO	5.40	7.13	7.79	5.80	7.27	6.65	6.18	7.04	6.94	6.49	7.00	5.36	5.02	5.10	5.26	5.40	5.19
ZnO	0.23	0.18	0.17	0.21	0.16	0.12	2.86	2.79	2.76	2.78	4.44	0.24	0.16	0.24	0.22	0.19	0.12
CaO	0.61	0.56	0.47	0.20	0.47	0.32	0.07	0.47	0.35	0.35	0.51	0.24	0.42	0.27	0.15	0.15	0.18
Na_2O	2.87	3.46	3.11	2.78	3.19	2.53	2.14	4.77	3.68	3.53	6.30	2.78	2.45	2.74	2.26	2.45	2.09
K_2O	0.20	0.25	0.20	0.19	0.22	0.19	0.05	0.59	0.27	0.24	0.59	0.17	0.19	0.21	0.17	0.19	0.17
F_{SIMS}	1.76	2.38	2.56	1.78	2.49	1.41	0.74	1.76	0.92	1.03	2.05	1.33	1.12	1.44	1.12	1.12	1.17
Li_2O_{SIMS}	3.74	3.28	3.59	3.60	3.41	3.56	3.18	1.91	2.77	2.87	2.39	3.76	3.56	3.69	4.06	3.97	3.90
H_2O_{SIMS}	1.08	0.97	1.01	1.18	0.99	1.23	1.77	1.19	1.38	1.32	1.09	1.39	1.48	1.16	1.80	1.63	1.59
O=F	0.74	1.00	1.08	0.75	1.05	0.59	0.31	0.74	0.39	0.43	0.86	0.56	0.47	0.61	0.47	0.47	0.49
Total	97.13	98.72	98.89	98.40	97.03	97.93	98.92	99.08	98.86	96.37	98.79	98.23	99.11	99.22	99.52	100.19	99.42
Si	8.00	8.00	8.00	8.00	8.00	8.00	8.00	8.00	8.00	8.00	8.00	8.00	8.00	8.00	8.00	8.00	8.00
Al	0.21	0.17	0.21	0.19	0.16	0.22	0.08	0.09	0.12	0.07	0.12	0.27	0.27	0.16	0.23	0.23	0.24
Mg	1.18	1.53	1.65	1.25	1.55	1.41	1.34	1.53	1.50	1.44	1.51	1.16	1.08	1.09	1.12	1.14	1.11
Ti	0.14	0.09	0.09	0.16	0.10	0.12	0.02	0.04	0.05	0.05	0.10	0.09	0.20	0.24	0.15	0.17	0.16
Fe^{2+}	1.22	1.17	1.00	1.04	0.47	0.74	0.90	0.55	0.22	0.25	0.56	1.55	1.50	1.23	1.72	1.77	1.43
Fe^{3+}	1.55	1.49	1.44	1.70	1.93	1.90	1.92	1.95	2.21	2.22	1.51	1.38	1.39	1.63	1.19	1.18	1.48
Mn^{2+}	0.09	0.08	0.08	0.08	0.07	0.07	0.14	0.13	0.13	0.14	0.08	0.09	0.09	0.09	0.08	0.08	0.07
Zn^{2+}	0.03	0.02	0.02	0.02	0.02	0.01	0.31	0.30	0.29	0.30	0.48	0.03	0.02	0.03	0.02	0.02	0.01
Li	0.58	0.46	0.51	0.56	0.70	0.53	0.29	0.41	0.48	0.53	0.64	0.43	0.45	0.53	0.49	0.41	0.50
Sum C	5.00	5.00	5.00	5.00	5.00	5.00	5.00	5.00	5.00	5.00	5.00	5.00	5.00	5.00	5.00	5.00	5.00
Li	1.62	1.44	1.54	1.52	1.27	1.52	1.56	0.71	1.12	1.18	0.76	1.76	1.61	1.61	1.84	1.86	1.74
Ca	0.10	0.09	0.07	0.03	0.07	0.05	0.01	0.07	0.05	0.06	0.08	0.04	0.06	0.04	0.02	0.02	0.03
Na	0.29	0.48	0.39	0.45	0.66	0.43	0.43	1.22	0.83	0.76	1.16	0.20	0.33	0.35	0.14	0.12	0.23
Sum B	2.00	2.00	2.00	2.00	2.00	2.00	2.00	2.00	2.00	2.00	2.00	2.00	2.00	2.00	2.00	2.00	2.00
Na	0.53	0.49	0.47	0.33	0.23	0.27	0.17	0.13	0.20	0.25	0.63	0.59	0.36	0.41	0.49	0.56	0.35
K	0.04	0.04	0.04	0.03	0.04	0.03	0.01	0.11	0.05	0.04	0.11	0.03	0.04	0.04	0.03	0.03	0.03
Sum A	0.57	0.53	0.51	0.36	0.27	0.30	0.18	0.24	0.25	0.29	0.74	0.62	0.40	0.45	0.52	0.59	0.38
F	0.81	1.08	1.15	0.81	1.13	0.64	0.34	0.81	0.42	0.48	0.95	0.61	0.51	0.65	0.51	0.50	0.53
OH	1.05	0.93	0.96	1.13	0.95	1.18	1.71	1.16	1.32	1.30	1.06	1.35	1.42	1.11	1.72	1.55	1.51
Sum O3	1.86	2.01	2.11	1.94	2.08	1.82	2.05	1.97	1.74	1.78	2.01	1.96	1.93	1.76	2.23	2.05	2.04
O.S.	0.56	0.56	0.59	0.62	0.80	0.72	0.68	0.78	0.91	0.90	0.73	0.47	0.48	0.57	0.41	0.40	0.51
Li_2O_{est}	3.78	3.15	3.56	3.94	4.14	3.96	3.34	2.19	3.19	3.29	2.20	3.43	3.65	3.81	4.00	3.64	4.12
H_2O_{est}	1.22	0.96	0.90	1.24	0.91	1.42	1.72	1.23	1.65	1.54	1.08	1.43	1.55	1.40	1.57	1.57	1.55
$^{M3}Li_{est}$	0.59	0.46	0.50	0.56	0.70	0.53	0.29	0.41	0.49	0.53	0.64	0.43	0.45	0.52	0.49	0.41	0.50
$^{M4}Li_{est}$	1.63	1.36	1.53	1.71	1.69	1.75	1.66	0.87	1.36	1.42	0.66	1.58	1.66	1.68	1.81	1.68	1.86
Sum A_{est}	0.58	0.46	0.50	0.55	0.70	0.53	0.28	0.40	0.49	0.53	0.63	0.43	0.45	0.52	0.49	0.41	0.50
$O.S._{est}$	0.51	0.59	0.63	0.53	0.66	0.57	0.66	0.70	0.71	0.72	0.78	0.52	0.44	0.46	0.50	0.48	0.48

(O.S.) is too high (*e.g.*, > 0.70) with respect to other points in the same rock sample. Thus, the sum of the oxides is too low, and the A-site occupancy is also very low. A comparison with the Li_2O values calculated according to the procedure discussed in the next section (Li_2O_{est}) shows that these features correspond to excessively low Li_2O contents in SIMS analyses. On the contrary, anomalous low O.S. values (*e.g.,* < 0.50) correspond to overestimation of the Li_2O content. The discrepancy between measured and estimated Li_2O values in Table 5b (omitting point 6 in sample C24) is ≤ 13 % rel, which is a good result when considering the strong compositional variability of the investigated samples. The six lines at the bottom of Table 5b show that more coherent and crystal-chemically reasonable results are obtained with our procedure, and that differences with Li_2O_{SIMS} are within their estimated accuracy. It is noteworthy that these changes mainly affect the estimate of ^{B}Li, whereas ^{C}Li is almost unaffected.

4. Cation ordering, crystal-chemical mechanisms and constraints

Octahedral site populations for the refined samples were calculated taking into account the unit formulae (Table 5a) as well as the refined site-scattering and mean bond-length values. Site assignments were based on previous knowledge on cation site-preference in amphiboles. Ti and all the trivalent cations (which however sum to < 2 apfu in all the samples) were assigned to the M2 site, due to the lack of evidence for partial dehydrogenation. Octahedral lithium (always < 1 apfu) was assigned to the

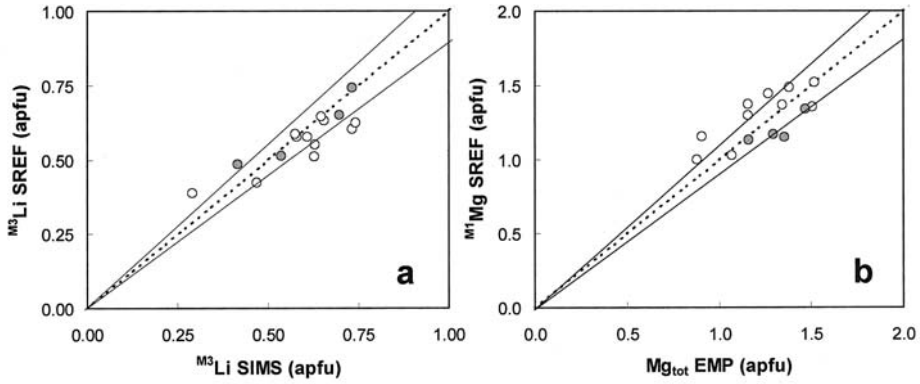

Fig. 1. Refined occupancy at the relevant sites *vs.* elemental abundance (in apfu) from chemical analysis for the 13 refined crystal. (a) octahedral Li, ordered at M3; (b) octahedral Mg, ordered at M1. Grey symbols refer to the Zn-rich crystals (sample C5). The inner lines represent ideal behaviour, the outer lines the ± 10 %rel. accuracy; esd are within the size of the symbols for Mg_{EMP}, Mg_{ref}, and Li_{ref}, and can be up to three times its size (at highest Li contents) for Li_{SIMS}.

M3 site, as suggested by previous studies (*e.g.*, Hawthorne *et al.*, 1994). However, the site preference of divalent cations (Mg, Mn, Fe^{2+}, and Zn) was the most critical issue. Structure refinements were done varying the relative occupancies (summing to 1) of the scattering curves for Fe^{2+} and Li^{+} at the M3 site. Therefore, the refined Li occupancy is correct if Fe^{2+} and Li^{+} are the only components, but it is the minimum Li content if the M3 site is occupied by Li and Zn (± Fe^{2+}), and the maximum Li content if the M3 site is occupied by Li, Mg, Mn (± Fe^{2+}). Figure 1a shows the excellent agreement between the refined Li occupancy at the M3 site and the ^{C}Li content in the unit formula. The Zn-rich crystals (grey circles) plot either close or to the left of the 1:1 line, suggesting that the M3 site is mostly occupied by Li, Fe^{2+} and perhaps Mn (*i.e.*, by the largest cations), and that Zn should thus partition itself between the M2 and M1 sites. An analogous argument can be applied for the M1 site, where the occupancy from the scattering curve of Mg^{2+} was refined against Fe^{2+}. Figure 1b shows that nearly all Mg enters the M1 site, and that only minor Zn enters the M1 site in the Zn-richest samples. Therefore, the site-preference of Zn in these amphiboles is M2 > M1. This conclusion supports the few evidences so far available. Hawthorne *et al.* (1996a) assigned Zn (up to 0.6 apfu) to the M2 site in Li-bearing fluoro-arfvedsonites found in miarolitic cavities in a pegmatitic phase of a riebeckite granite at Hurricane Mountain (New Hampshire). In Li-bearing amphiboles from peralkaline granites at Strange Lake (Quebec), Hawthorne *et al*. (2001) related the increase in the Zn content to the culmination of the agpaitic trend of crystallization, and concluded that Zn (up to 0.12 apfu) should be disordered among at least two of the three octahedral sites.

Two further aspects of cation ordering in Li-rich amphiboles deserve some comments. The first concerns the significant differences in the coordination of the various B cations. Lithium occurs in a position (M4') closer to the strip of octahedra than that occupied by sodium and calcium (M4), and assumes a [5+1]- or a [6]-fold coordination in orthorhombic and in monoclinic amphiboles, respectively. Because diffraction averages over the whole crystal volume, the presence of different B sites results in a complex shape of the electron density that strongly depends on the relative percentages of the two types of cations. This feature is typical of all pyroxenes and amphiboles in which cations with different sizes occur at the same site (M2 and M4, respectively), and has been already commented in a large number of papers. In all these cases, the use of a single atom position with a strongly anisotropic displacement factor does not allow a correct estimate of the scattering power. Best results are obtained when using a split model (with two anisotropic or with one anisotropic and one isotropic displacement factor, depending on the shape of the maximum). However, these models may still fail to account for some details of the electron density; therefore, the refined site-scattering values at the B-group sites may be lower than those calculated from the formulae, suggesting a higher ^{B}Li content. This is often the case, as shown in Table 5a.

Analogously, the A cations in Li-rich amphiboles move well away from the central position. In amphiboles, the splitting of the A cations between the A2 and the A*m* positions is also well known, and a complete analysis of their ordering as a function of the composition of the other sites has been given in Hawthorne *et al.* (1996c). In Li-rich amphiboles, the A cations occur at a particularly off-centred A*m* position. Also in this case, the very irregular shape of the electron-density may lead to underestimation of the scattering power at the A sites (Table 5a).

5. A method to calculate lithium content and partitioning from EMP results

The above discussion, and the use of all the data available for Li-bearing amphiboles obtained at the CNR-IGG in Pavia, provide criteria to calculate reliable Li_2O contents, and also reliable Li partitioning, even in the absence of SIMS analyses. This procedure holds only in the absence of partial dehydrogenation, and should be modi-

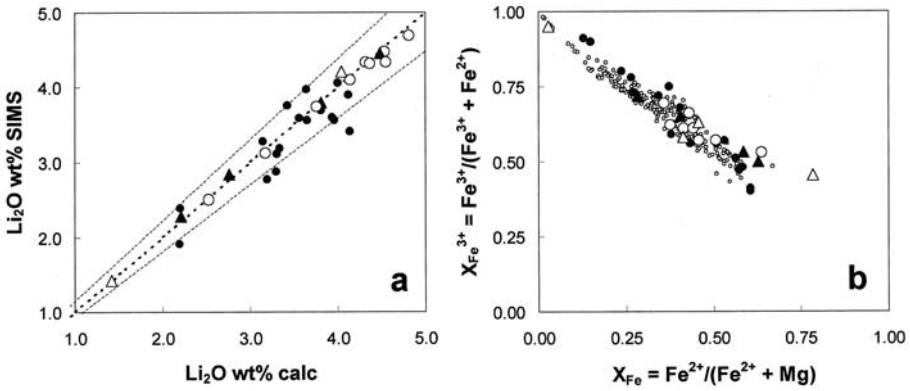

Fig. 2. Validation of the procedure proposed to calculate Li_2O wt% and partition Li between the B- and C-group sites in amphiboles. (a) the agreement between the measured and calculated Li_2O values is within the experimental accuracy (~ 10-15 %). (b) The O.S. values calculated in the absence of Li_2O and H_2O analyses are strictly coherent to those obtained from EMP + SIMS analyses. Black triangles: the four new Li-rich end-members; open triangles: former Li-rich end-members; large open circles: the other crystals; black circles: EMP + SIMS analyses on thin sections; small open circles: EMP analyses from thin sections. Lines as in Fig. 1.

fied in the case of amphiboles from peralkaline granites, such as those studied by Hawthorne *et al.* (1993), which crystallised under highly oxidizing conditions. The available criteria are:

(1) the tetrahedral sites are completely or almost completely occupied by Si;
(2) the H_2O content can be calculated so as to obtain (OH + F) = 2 apfu
(3) high charged cations (R^{3+} and R^{4+}) are ordered at the M2 site, so that $R^{3+} + R^{4+}$ must be ≤ 2.0 apfu (if partial dehydrogenation is present, some Ti should enter the M1 site, and the sum $R^{3+} + R^{4+}$ might exceed 2.0 apfu);
(4) Fe^{2+} and Mg contents at the B-group sites are nil or negligible.

Therefore, unit formulae can be obtained on the basis of 24 (O, F, OH) atoms, with H_2O wt% calculated in such a way that F + OH = 2 apfu. In the first attempt, Fe^{3+} should be fixed at 2 - Al – Ti apfu, this value representing the maximum Fe^{3+} content. Li_2O wt% must be calculated taking into account charge constraints, provided only that the sum of the wt% oxides is reasonably close to 100 %. At this point, ^{C}Li is assumed to be equal to 5 - $(Fe, Al, Mn)^{3+}$ - Ti^{4+} - $(Fe, Zn, Mg, Mn)^{2+}$, this being the minimum ^{C}Li content (because Fe^{3+} is maximum). Crystal-chemical analysis suggests that the (Na + K) occupancy at the A site is at least equal to ^{C}Li. If this constraint is not obeyed, the Fe^{3+} content calculated as described above must be lowered, and/or the Li_2O wt% must be increased to fulfil all the crystal-chemical requirements previously discussed.

This procedure was first tested in the case of the 30 EMP + SIMS analyses reported in Table 5; the agreement between the measured and the calculated Li_2O wt% values is within 10 % for most samples (Fig. 2a). The procedure was subsequently tested on the ~ 200 EMP analyses performed on thin sections at the Universidad Complutense in Madrid. The O.S. values in the resulting unit formulae are fully coherent with the values obtained for the crystals from the same rock sample that could been analysed by EMP and SIMS (Fig. 2b). We should point out that the trend observed in Fig. 2b also implies a regular decrease in fO_2 during the cooling process.

6. Discussion

All the analyses available for Li-rich amphiboles from the Eastern Pedriza Massif are plotted in Fig. 3, where the amounts of lithium entering the B- and the C-group sites are compared. It is clear that the analysed samples cover almost all the allowed compositional space, and that no miscibility gap is present in the solid-solution between sodium and lithium at the B-group sites, notwithstanding the large difference in the ionic radii (1.02 *vs.* 0.76 Å in [6]-fold and 1.18 *vs.* 0.92 Å in [8]-fold coordination, respectively). This is particularly interesting, because the presence of Na and Ca in amphiboles of the Mg-Fe-Mn-Li group (and *vice versa*) is always very scarce in nature. Actually, the nature of the B-group sites cations is the criterion selected to distinguish the various amphibole groups for nomenclature purposes.

In all these analysed samples, the ^{M3}Li content is always at least equal to the A-sites occupancy. This constraint was first noted and discussed by Hawthorne *et al.* (1994) based on bond valence calculations for leakeite; these authors however noted that it does not correspond to a real exchange vector. The Li-rich amphiboles found at the Pedriza Massif now allow a better crystal-chemical explanation based on cation ordering.

In the amphibole structure, the M3 site coordinates four O1 sites (occupied by O^{2-}) and two O3 sites (occupied by OH, F, or O^{2-}). The heterovalent substitution $^{M3}Li\ ^{M3}Fe^{2+}_{-1}$ therefore implies the need for further bond-strength contribution to these O sites, which must be supplied by the other coordinated cations, mostly by a large trivalent cation (Fe^{3+}) at the adjacent M2 site (which in turn coordinates two O1, two O2 and two O4 sites). However, the O2 and the O4 sites are also coordinated with the M4 site, and bond valence calculation for O4 always give values lower that 2

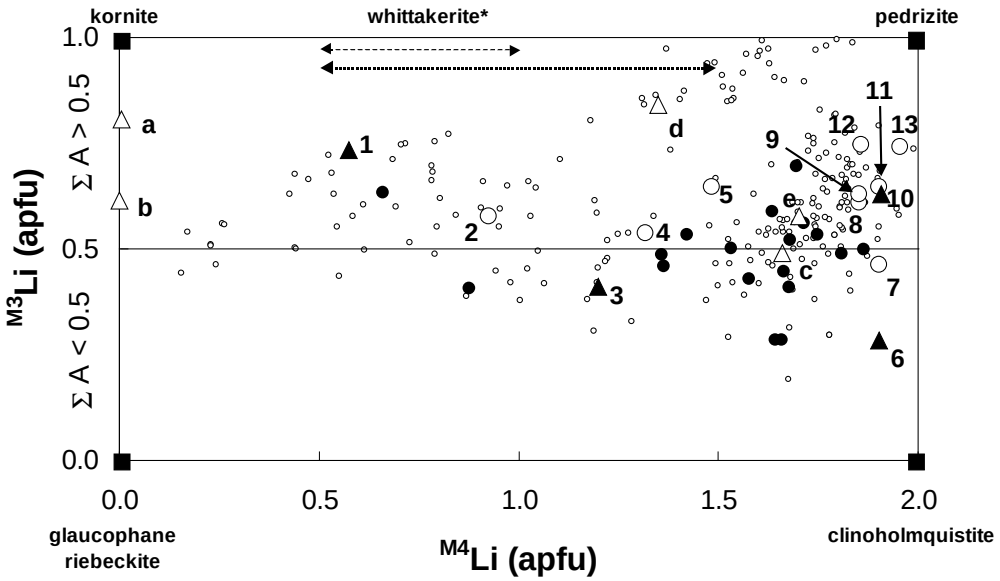

Fig. 3. The solid solution between Li and Fe^{2+} at the M3 site and between Li and Na at the M4 site in the Li-rich amphiboles from Pedriza. The relevant root-names are shown, and the complete names are obtained by combining the proper sodic, ferro and ferri prefixes. Same symbols as in Fig. 2. a = Hawthorne *et al.* (1992); b = Hawthorne *et al.* (1996b); c = Caballero *et al.* (1998); d = Oberti *et al.* (2000); e = Caballero *et al*. (2002). * The root name whittakerite has been approved by IMA-CNMMN who are considering whether the boundaries shown should be approved: dashed line = Leake *et al.* (1997), dotted line = pending proposal (Leake, pers. com.).

vu. Accordingly, Fig. 4a shows a strong decrease in the apical T1-O1 distance (and thus an increasing bond-strength contribution of the T1 cations) as a function of increasing ^{M3}Li content in all the Li-rich amphiboles for which a structure refinement is available. The refined site-scattering values at M3 are used in Fig. 4 and Fig. 5 as an inverse measure of the ^{M3}Li content because they represent experimental data that are free of any bias which might result from erroneous assignment of site populations. The need for bond-strength contribution from the T1 cation may also explain the absence of $^{[4]}Al^{3+}$ in Li-rich amphiboles. On the contrary, the three basal distances (T1-O5, T1-O6, and T1-O7) lengthen as a function of the ^{M3}Li content, thus maintaining the <T1-O> distance constant as already noted in Table 3 and in previous papers on ^{M3}Li-rich amphiboles. Also, there is a change in the geometry of the six-membered ring of tetrahedra. In particular, the O6-O7-O6 angle decreases sharply, thus pushing the O6 oxygen atoms closer to the A*m* site, and increasing the bond-strength contribution from A-site cations (Fig. 4b).

Figure 5a shows the 1:1 correlation between the refined site-scattering values at the M3 site and the A-sites occupancy, which implies that ^{M3}Li locally couples with a monovalent cation at the next-nearest-neighbour A*m* site (short-range order). Figure 5b shows the extent of the off-centring of the A cations as a function of ^{M3}Li (and thus of A-sites occupancy). Therefore, the bond-strength requirements of the basal oxygen atoms of the tetrahedra are a stringent constraint. The maximum off-centring is observed for the smaller Na^+ ion in samples with ^{M3}Li:^{A}(Na,K) ratio

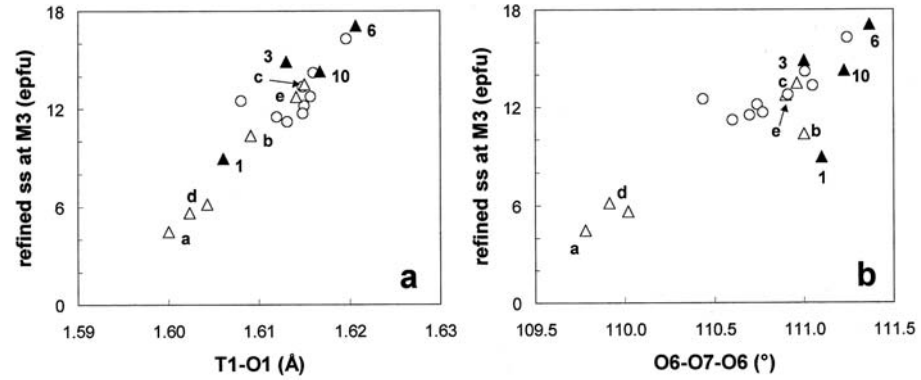

Fig. 4. Lithium incorporation at the M3 site and crystal-chemical behaviour of T cations. (a) Increasing bond-strength contribution *via* the O1 oxygen; (b) shrinking of the six-membered ring of tetrahedra.

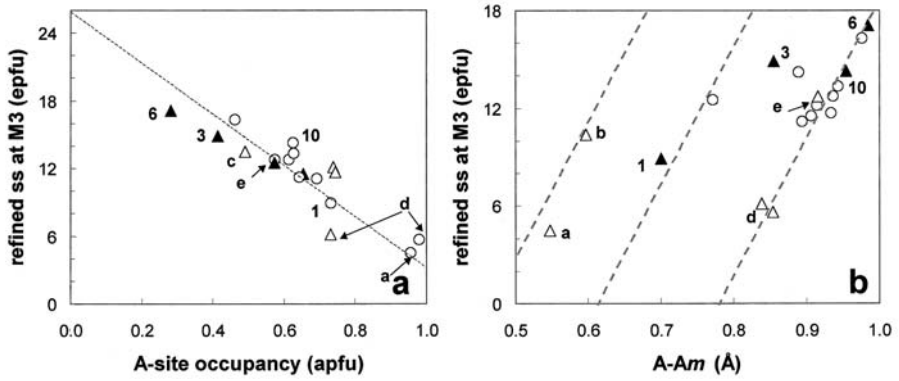

Fig. 5. Lithium incorporation at the M3 site and crystal-chemical behaviour of A-sites cations. (a) 1:1 correlation between ^{M3}Li and the A-site occupancy; (b) A*m* off-centring is an inverse function of the total occupancy and of the K^+ content (dashed lines drawn at 0.03, 0.13, and 0.23 K apfu). Sample c could not be included in Fig. 5b because a different model was used for the A-site refinement.

close to1:1, whereas increasing contents of the larger K^+ ion and of the ^{M3}Li:^{A}(Na,K) ratio correspond to decreasing values of the A-A*m* separation.

A direct relation between ^{M3}Li and ^{M3}F (which is bonded to M3) is also observed in Table 5. The presence of F at the O3 site is another factor favouring ordering of the A cations at the A*m* site, which would be affected by steric hindrance between A*m* and H (Hawthorne *et al*., 1996c). As a matter of fact, the occupancy of the A*m* site is complementary to the OH content at the O3 site (Table 5). On the contrary, partial dehydrogenation at the O3 site, which would require a further bond strength contribution by the adjacent cations (at the M1 and M3 sites), is prevented in ^{M3}Li-bearing amphiboles, especially when the ^{M3}Li:^{A}(Na,K) ratio is close to 1:1. The only reported ^{M3}Li-rich samples with partial dehydrogenation (Hawthorne *et al.*, 1993) have been found in high-*T* and high fO_2 environments, and all have an alkali content at the A-site close to 1 apfu. In their case, there is also a local ^{M3}Li-$^{O3}O^{2-}$ avoidance, which implies that ^{M3}Li is < 1 – $^{O3}O^{2-}$.

All the available data allow some further conclusions to be drawn. The total lithium content in amphiboles must depend primarily on the composition of the coexisting fluid during their crystallisation. However, the ^{M3}Li content is directly related to the Mg number, and thus should be higher at higher temperatures of crystallization. This conclusion is further supported by analytical core-to-rim traverses in crystals of suitable dimensions from sample C5. On the contrary, the ^{M4}Li content is inversely related to the Mg number in the studied samples. Accordingly, the ^{M3}Li-rich ^{M4}Li-free sodic amphiboles from peralkaline granites (Hawthorne *et al*., 1993) formed under much higher *T* conditions.

Some hints can also be obtained on the petrological and geochemical evolution of epysienites in the Eastern Pedriza Massif. The compositional variations observed in the various amphiboles examined in sample C5 define a trend from leakeite towards the boundary between pedrizite and clinoholmquistite; the same kind of evolution, albeit in minor amounts, is recorded in sodic-ferripedrizites from sample C3. This evidence can be interpreted primarily in terms of an open metasomatic systems, where a progressive increase of the Li^+/Na^+ ratio in the fluid (lithium being incorporated into the B sites) is coupled with a decrease in the crystallisation temperature. Calculations were performed assuming a closed system for fluids equilibrated with granites at the highest salinities compatible with fluid inclusions data (SUPCRT92, Johnson *et al.*, 1992; Caballero, 1999). They indicate that the Li^+/Na^+ ratio increases while *T* decreases in a range (600-430ºC) around the estimated value of 520ºC; the lower limit of this range increases for a lower given salinity.

The rock samples containing the ^{B}Li richest amphiboles (C2, C20-C24, and C4) define a transition from pedrizite to clinoholmquistite, in which ^{B}Li is nearly constant or decreases slightly with the Mg number, whereas ^{M3}Li increases with the Mg number (a *T* dependent substitution).

Acknowledgements: Simona Bigi kindly helped during EMP analyses at the Università di Modena; funding by CNR is also acknowledged. Thanks are also due to the staff of the C.A.I. "Luis Bru" (U.C. Madrid) for assistance in preliminary electron-microprobe analyses.

References

Armstrong, J.T. (1988): Quantitative analysis of silicate and oxide minerals. Comparison of Monte-Carlo, ZAF and Phi-Rho-Z procedures. *Microbeam Analyses*, **23**, 239–246.

Caballero, J.M. (1993): Las episienitas de la Sierra de Guadarrama: Un caso singular de alteración hidrotermal de edad post-hercínica, 313 p. PhD. Thesis, Universidad Complutense de Madrid.

— (1999): Modelización del proceso de episienitización (decuarcificación-albitización): Formulación cinética y transporte advectivo en medio continuo. *Estudios Geológicos*, **55**, 9–26.

Caballero, J.M., Monge, A., La Iglesia, A., Tornos, F. (1998): Ferriclinoferroholmquistite, $Li_2(Fe^{2+},Mg)_3Fe^{3+}_2Si_8O_{22}(OH)_2$, a new ^{B}Li clinoamphibole from the Pedriza Massif, Sierra de Guadarrama, Spanish Central System. *Am. Mineral.*, **83**, 167–171.

Caballero, J.M., Oberti, R., Ottolini, L. (2002): Ferripedrizite, a new monoclinic ^{B}Li amphibole end-member from the Eastern Pedriza Massif, Sierra de Guadarrama, Spain, and a restatement of the nomenclature of Mg-Fe-Mn-Li amphiboles. *Am. Mineral.*, **87**, 976–982.

Donovan, J.J. & Rivers, M.L. (1990): PRSUPR – A PC based automation and analysis software package for wavelength-dispersive electron-beam microanalysis. *Microbeam Analysis*, **25**, 66–68.

González-Casado, J.M., Caballero, J.M., Casquet, C., Galindo, C., Tornos, F. (1996): Palaeostress and geotectonic interpretation of the Alpine Cycle onset in the Sierra del Guadarrama (eastern Iberian Central System), based on evidence from episyenites. *Tectonophysics*, **262**, 213–229.

Hawthorne, F.C., Oberti, R., Ungaretti, L., Grice, J.D. (1992): Leakeite, $NaNa_2(Mg_2Fe^{3+}_2Li)Si_8O_{22}(OH)_2$, a new alkali amphibole from the Kajlidongri manganese mine, Jhabua district, Madhya Pradesh, India. *Am. Mineral.*, **77**, 1112–1115.

Hawthorne, F.C., Ungaretti, L., Oberti, R., Bottazzi, P., Czamanske, G. K. (1993): Li: an important component in igneous alkali amphiboles. *Am. Mineral.*, **78**, 733–745.

Hawthorne, F.C., Ungaretti, L., Oberti, R., Cannillo, E. (1994): The mechanism of $^{[6]}$Li incorporation in amphiboles. *Am. Mineral.*, **79**, 443–451.

Hawthorne, F.C., Oberti, R., Ottolini, L., Foord, E.E. (1996a): Lithium-bearing fluor-arfvedsonite from Hurricane Mountain, New Hampshire: a crystal-chemical study. *Can. Mineral.*, **34**, 1015–1019.

Hawthorne, F.C., Oberti, R., Ungaretti, L., Ottolini, L., Grice, J.D., Czamanske, G.K. (1996b): Fluor-ferro- leakeite, $NaNa_2(Fe^{2+}_2Fe^{3+}_2Li)Si_8O_{22}F_2$, a new alkali amphibole from the Canada Pinabete Pluton, Questa, New Mexico, U.S.A. *Am. Mineral.*, **81**, 226–228.

Hawthorne, F.C., Oberti, R., Sardone, N. (1996c): Sodium at the A site in clinoamphiboles: the effects of composition on patterns of order. *Can. Mineral.*, **34**, 577–593.

Hawthorne, F.C., Oberti, R., Cannillo, E., Ottolini, L., Roelofsen, J., Martin, R.M. (2001): Li-bearing amphiboles from the Strange Lake peralkaline granite, Quebec. *Can. Mineral.*, **39**, 1161–1170.

Johnson, J.W., Oelkers, E.H., Helgeson, H.C. (1992): SUPCRT92: A software package for calculating the standard molal thermodynamic properties of minerals, gases, aqueous species and reactions from 1 to 5000 bars and 0 to 1000ºC. *Computers and Geosciences*, **18**, 899–947.

Leake, B.E, Woolley, A.R, Arps, C.E.S., Birch, W.D., Gilbert, M.C., Grice, J.D., Hawthorne, F.C., Kato, A., Kisch, H.J., Krivovichev, V.G., Linthout, K., Laird, J., Mandarino, J.A, Maresch, W.V, Nickel, E.H., Rock, N.M.S., Schumacher, J.C., Smith, D.C., Stephenson, N.C.N., Ungaretti, L., Whittaker, E.J.W., Guo, Y. (1997): Nomenclature of amphiboles: Report of the subcommittee on amphiboles of the International Mineralogical Association, Commission on New Minerals and Mineral Names. *Am. Mineral*, **82**, 1019–1037.

Oberti, R., Ungaretti, L., Cannillo, E., Hawthorne, F.C., Memmi, I. (1995): Temperature-dependent Al order-disorder in the tetrahedral double chain of *C*2/*m* amphiboles. *Eur. J. Mineral.*, **7**, 1049–1063.

Oberti, R., Caballero, J.M., Ottolini, L., López-Andrés, S., Herreros, V. (2000): Sodic-ferripedrizite, a new monoclinic amphibole bridging the magnesium-iron-manganese-lithium and the sodium-calcium groups. *Am. Mineral.*, **85**, 578–585.

Ottolini, L. & Hawthorne, F.C. (2001): SIMS ionization of hydrogen in silicates: a case study of kornerupine. *J. Anal. Atomic Spectrom.*, **16**, 1266–1270.

Ottolini, L. & Oberti, R. (2000): Accurate quantification of H, Li, Be, B, F, Ba, REE, Y, Th and U in complex matrixes: A combined approach based on SIMS and Single-Crystal Structure Refinement. *Analyt. Chem.*, **72**, 3731–3738.

Ottolini, L., Bottazzi, P., Vannucci, R. (1993): Quantification of Li, Be and B in silicates by secondary ion mass spectrometry using conventional energy filtering. *Analyt. Chem.*, **65**, 1960–1968.

Villaseca, C. & Pérez-Soba, C. (1989): Fenómenos de alcalinización en granitoides hercínicos de la Sierra de Guadarrama (Sistema Central). *Cuadernos Laboratorio Xeolóxico Laxe*, **14**, 201–212.

Received 16 January 2002
Modified version received 24 June 2002
Accepted 28 October 2002